Quenching and restoring of the A 2Π cationic state in resonant Auger electron spectra of CO in the vicinity of the O 1s 2π resonance

Quenching and restoring of the $A\ ^2\Pi$ cationic state in resonant Auger electron spectra of CO in the vicinity of the O $1s \rightarrow 2\pi$ resonance

R. Feifel,[1,2,*] T. Tanaka,[3] M. Hoshino,[3] H. Tanaka,[3] Y. Tamenori,[4] V. Carravetta,[5,2] and K. Ueda[2,†]

[1]*Department of Physics, Uppsala University, Box 530, SE-751 21 Uppsala, Sweden*

[2]*Institute of Multidisciplinary Research for Advanced Materials, Tohoku University, Sendai 980-8577, Japan*

[3]*Department of Physics, Sophia University, Tokyo 102-8554, Japan*

[4]*Japan Synchrotron Radiation Research Institute, Sayo-gun, Hyogo 679-5198, Japan*

[5]*Area of Research, IPCF-CNR, via Moruzzi 1, 56124, Pisa, Italy*

(Received 22 September 2006; revised manuscript received 27 October 2006; published 29 December 2006)

The evolution of the vibrational intensity distribution of the singly ionized $A\ ^2\Pi$ state in CO is experimentally examined for photon energy detunings below the adiabatic 0-0 transition of the O $1s \rightarrow 2\pi$ resonance. We have found a strong suppression of the entire vibrational fine structure of this state, leading to its almost complete quenching for certain excitation energies, followed by a partial restoring for larger values of negative photon energy detuning. Our observation, that cannot be rationalized by the known model of a vibrational collapse for energy detuning, may be explained in terms of a Fano interference between the direct and resonant photoionization channels in the presence of strong lifetime vibrational interference.

PACS number(s): 33.80.Eh

I. INTRODUCTION

Resonant Auger electron spectroscopy performed under "Raman conditions" [1,2] has become a field of wide interest during the last few years [3–6]. Raman conditions imply that the photon energy bandwidth of the excitation source is smaller than the natural lifetime width of the intermediate core-excited state. This type of experiment is today possible for a variety of core levels, like, for example, the C $1s$, N $1s$, O $1s$, and F $1s$ edges, in particular at third-generation high-brilliance synchrotron-radiation light sources, where high-resolution and high-photon flux soft x-ray beam lines are available for this purpose.

In such experiments, several fundamental effects in soft x-ray atomic and molecular physics have been revealed. As examples, ultrafast dissociation of core-excited molecules (see, e.g., Ref. [7]), the related phenomenon of Doppler splitting of fragment peaks [8–10] and the formation of a continuum-continuum interference hole [11] can be mentioned. Of particular interest is lifetime vibrational interference (LVI) [12–17] which can result for photon frequency detuning and under certain circumstances in the collapse of vibrational fine structure [18,19] and the interference quenching of a single vibrational line [20,21]. The latter phenomena are expected to occur if the equilibrium bond distances of the neutral ground and singly ionized final states approximately coincide [18–21]. All these effects are essentially understood as resonant phenomena within the framework of the established duration time concept of the scattering process [22].

The interference between the nonresonant and resonant photoionization processes [23–25] may also play a significant role, depending on the relative strengths of the various channels involved (see e.g. Refs. [20,26–29]). In a recent study, we observed such interference effects in electron spectra of CO for selective vibrational excitations across the O $1s \rightarrow 2\pi$ resonance [30], i.e., for positive photon energy detuning with respect to the adiabatic 0-0 transition at 533.42 eV. In this case the interference between the nonresonant and resonant channels was found to be important for a detailed understanding of the alterations in the vibrational intensity distributions of the $X\ ^2\Sigma^+$ and $A\ ^2\Pi$ cationic states.

In the present work, we examine the evolution of the vibrational intensity distribution of the singly ionized $A\ ^2\Pi$ state when the photon energy is tuned below the adiabatic 0-0 transition of the O $1s \rightarrow 2\pi$ resonance (i.e., negative photon energy detuning; cf. above and Ref. [30]). A strong suppression of the entire vibrational fine structure of this state is found, leading to its almost complete quenching for certain excitation energies. The vibrational progression appears again for even larger detunings. In order to get a deeper insight into the mechanism behind this behavior, we have performed various sets of numerical simulations, taking lifetime vibrational interference and the interference between the direct and resonant channels into account. As will be seen, our observations can be explained primarily in terms of a Fano interference between the direct and resonant photoionization channels.

II. EXPERIMENTAL DETAILS

The experiment was carried out using linearly polarized synchrotron radiation from the high-resolution photochemistry beamline 27SU [31,32] at SPring-8 in Japan. The polarization vector $\mathcal{E}$ of the undulator light may be set to horizontal (first harmonic) or vertical (0.5th harmonic) at this beamline [33,34]. The spectra were measured using a high-resolution electron spectrometer employing a hemisperical electron-energy analyzer (Gammadata Scienta SES-2002) fitted with a gas cell. The lens axis is in the horizontal direction, at right angles to the photon beam direction [35]. In this

*E-mail address: raimund.feifel@fysik.uu.se

†E-mail address: ueda@tagen.tohoku.ac.jp

arrangement, the electron spectra recorded with horizontal and vertical polarization correspond to the electron emission parallel and perpendicular to the $\mathcal{E}$ vector, respectively. The monitor of the photon flux for the normalization is made by two drain currents on the last refocusing mirror and after the gas sample. All spectra were normalized to the data acquisition time, the gas pressure, and the photon flux. Spectra corrected for anisotropic electron emission were constructed by combining the 0° and 90° spectra measured at the same photon energy according to the following equation, which assumes 100% linear polarization:

$$I(54.7°) = I(0°) + 2 \times I(90°). \tag{1}$$

Spectra of this type, usually referred to as "angle-integrated" or "magic angle" (54.7°) spectra, will be discussed below. The degree of linear polarization was measured by studying the Ne 2s and 2p photolines, and was found to be larger than 0.98 for the current optical settings [36], which justifies the assumption that the radiation is linear polarized. The monochromator bandpass was set to 67 meV full width at half maximum (FWHM), the electron spectrometer bandpass to 63 meV, and the inhomogeneous Doppler broadening due to thermal motion of the sample molecules is estimated to be around 54 meV, resulting in a total experimental linewidth for the electron spectra of around 107 meV. Electron spectra were recorded in the vicinity of the O $1s \rightarrow 2\pi$ resonance in CO. The photon energy calibration was made by measuring the total ion yield (TIY) with the ion detector which collects ions ejected to 4π sr using the DC field, and comparing to published absorption spectra [37,38]. The photon energy determination is found to be accurate to within ±40 meV. All electron spectra were calibrated relatively to the lowest vibrational level of the singly ionized $X\,^2\Sigma^+$ state in CO with a binding energy of $E_{\mathrm{Bin}} = 14.014$ eV according to Ref. [39]. CO gas was commercially obtained with a stated purity of >99.99%.

III. RESULTS AND DISCUSSION

In the left panel of Fig. 1 we present, in overview form, normalized resonant Auger electron spectra incorporating the first three outermost singly ionized $X\,^2\Sigma^+$, $A\,^2\Pi$, and $B\,^2\Sigma^+$ states of CO reached by participator decay. They were recorded for a series of selected excitation energies, starting on top of the adiabatic 0-0 transition (533.42 eV) of the O $1s \rightarrow 2\pi$ resonance, and going gradually toward lower photon energies. As can be seen, there are no significant changes in the intensity distribution of the $B\,^2\Sigma^+$ state (save for the spectrum measured at −11 eV where a strong contribution from second order light is present in this part of the spectrum). The small resonant contribution compared to the strength of the direct channel thus seems of little importance in this case.

For the $X\,^2\Sigma^+$ state a long vibrational progression (up to $\sim \nu'' = 8$) is visible in the spectrum excited on top of $\nu' = 0$ of the intermediate state. Most of this progression has essentially vanished in the spectra measured at −0.4 eV and further below the resonance, and the remaining intensity distribution is reminiscent of that of the direct valence
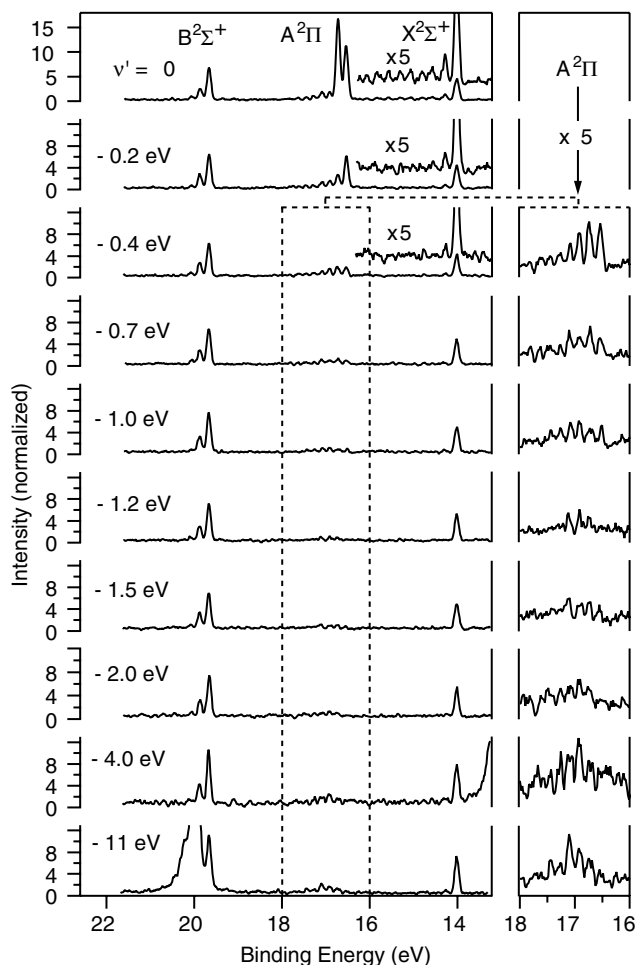

FIG. 1. Left panel: Normalized resonant Auger electron spectra of the singly ionized $X\,^2\Sigma^+$, $A\,^2\Pi$, and $B\,^2\Sigma^+$ final states of CO measured for selected photon energies in the vicinity of the O $1s \rightarrow 2\pi$ resonance. Right panel: blow-up of the $A\,^2\Pi$ state measured for photon energy detunings of −0.4 eV and further below the resonance.

photoelectron spectrum [39]. This type of behavior has been reported earlier for the same state by Sundin *et al.* [18] for photon energy detunings below the adiabatic transition of the C $1s \rightarrow 2\pi$ resonance (287.40 eV), where it was associated with a collapse of the vibrational quantum structure due to the shortening of the scattering duration time. Since the requirement for the occurrence of the collapse effect is that the equilibrium bond distances of the potential curves of the neutral ground and the singly ionized final states approximately coincide [18], the observation of such behavior in the vicinity of the O $1s \rightarrow 2\pi$ resonance is not unexpected. It should be noted, however, that the "collapse model" was developed on the assumption of a complete neglecting of the direct photoionization contribution to the cross section [18], while this contribution cannot be neglected in the present case [30] and would be needed to be accounted in a complete description of the observation made here.

For the $A\,^2\Pi$ state intensive vibrational progressions can be seen in Fig. 1 which vary strongly for excitation energies close to the resonance. This behavior can most likely be

TABLE I. Spectroscopic constants for the initial, intermediate, and the A $^2\Pi$ and B $^2\Sigma^+$ states [30,41] involved in the present study: ω_e is the vibrational frequency, $\omega_e x_e$ the anharmonicity, and R_e is the equilibrium bond distance.

	CO		CO$^+$	
	Ground State	O $1s \rightarrow 2\pi$	(A $^2\Pi$)	(B $^2\Sigma^+$)
ω_e (meV)	269.020	167	193.671	215.011
$\omega_e x_e$ (meV)	1.648	1.6	1.678	3.463
R_e (Å)	1.1283	1.288	1.2437	1.1687

attributed to the influence of the intermediate resonant state via lifetime vibrational interference (see also below). At excitation energies further away from the resonance, the entire vibrational progression decreases drastically in intensity until it has almost completely vanished at $\sim$$-1.2$ eV photon energy detuning. Thereafter it starts to appear again as can be seen from the blow-up of this state displayed in the right panel of Fig. 1. It is worth noting that for very large detuning values the relative height of the A state band would be expected to be much stronger, since it is $\sim$50% of the intensity of the $\nu''=0$ vibrational level of the B state in the 60 eV photoelectron spectrum [40], a ratio that is also predicted by calculations in the high energy region of the O $1s \rightarrow 2\pi$ transition [28]. Since the equilibrium bond distances of the neutral ground state and the A $^2\Pi$ state are substantially different (see Table I below), this peculiar behavior cannot be explained in terms of the collapse effect or an interference quenching of individual vibrational lines as discussed before in Refs. [18–21] for other electronic states.

For these reasons, we performed various sets of numerical simulations of the A $^2\Pi$ state based on the Kramers-Heisenberg equation [12,13] including the direct channel [27,29,30], which accounts for both lifetime vibrational interference and the interference between the direct and resonant channels:

$$I_f(\omega) = \left| D\langle f|0\rangle + M \sum_n \frac{\langle f|n\rangle\langle n|0\rangle}{\omega - \omega_{n0} + i\frac{\Gamma}{2}} \right|^2. \quad (2)$$

Here, the term $D\langle f|0\rangle$ stands for the direct photoionization to the final cationic state, $|0\rangle$, $|n\rangle$, $|f\rangle$ denote vibrational wave functions of the initial ground state, intermediate core-excited state, and final ionic state, respectively, and $|M|$ is the electronic transition moment for the Auger resonant Raman process under consideration. Γ is the lifetime width of the core-excited state, ω_{n0} is the energy of the core-excited vibrational state $|n\rangle$ relative to the ground vibrational state $|0\rangle$, and ω is the photon energy.

The vibrational wave functions $|0\rangle$ and $|f\rangle$ were calculated using spectroscopic constants from Huber and Herzberg [41], and the vibrational wave functions $|n\rangle$ were calculated using the spectroscopic constants obtained in our previous study [30]. Table I summarizes these parameters. Furthermore, we used an intermediate state lifetime width Γ of 156 meV for the simulations [30]. The photon bandwidth as well as the

spectrometer broadening were chosen according to the experimental conditions.

The remaining parameters to be determined are, M and D, or alternatively a ratio $|D/M|^2$ and an intensity scaling factor $|D|^2$. Considering the relatively narrow photon energy range examined in the present experiment, it is reasonable to assume that both M and D do not vary appreciably, as was also predicted by previous calculations in the high energy electronic continuum [28]. A dependence of the direct and resonant photoionization amplitude on the molecular geometry, implicitly neglected by adopting Eq. (2), may also be considered of minor importance because of the high energy of the emitted electron. We have then chosen D/M=const. in the application of Eq. (2). This ratio was determined by a qualitative fit of the simulated spectra to the experimental ones for a detunig between 0 and -11 eV. Allowing for a small photon energy inaccuracy in the experimental data (± 40 meV), we found $D/M=+0.84$. Furthermore, we also considered the case $D=0$ and M=const., which corresponds to pure LVI simulations, neglecting deliberately the direct channel.

Figure 2 shows the results of all these simulations alongside the experimental data, where the left intensity scale belongs to the experimental spectra, and the right intensity scale belongs to the numerical results. The experimental spectra are background corrected in order to allow for a direct comparison to the numerical results. In addition to the normalized intensity scale chosen, we included also parts of the B state (in particular $\nu''=1$) as an internal reference for comparison of relative intensities (for this state we found $D/M \sim 8.16$; see also the discussion of the B-state progression from above). As we can see, the numerical results obtained for $D=0$ resemble rather closely the experimental vibrational intensity distribution of the A state up to at least -0.4 eV detuning below the resonance, which suggests that the A-state progression is substantially influenced by LVI at these photon energies. By going further away from the resonance, however, the vibrational progression calculated according to pure LVI dies off continuously until it is not discernible anymore, in particular at -11 eV detuning, which stands in clear contrast to the experimental observation made. This is expected, since the direct channel must become more and more important the further away from the resonance. Hence, simulations which explicitly account for the direct channel according to Eq. (2), i.e., D/M=const., should give an improvement. The results of such simulations are displayed in the third panel from the left in Fig. 2 and in
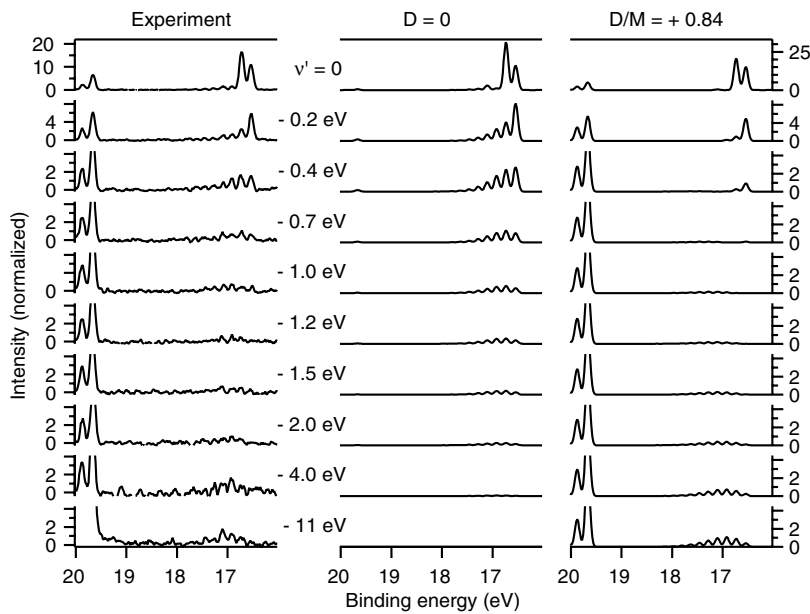
FIG. 2. Normalized resonant Auger electron spectra of the $A\,^2\Pi$ state in comparison to various sets of numerical simulations performed as explained in the text. Left intensity scale belongs to the experimental results, right intensity scale belongs to the numerical results.

greater detail in Fig. 3 where the theoretical spectra are presented as bar diagrams for a more clear comparison with the experimental profiles (background corrected). The spectrum calculated for $\nu'=0$ excitation resembles its experimental counterpart well, while the spectra calculated for −0.2, −0.4, and −0.7 eV detuning give only a qualitative description of the rapid quenching of the vibrational structure. The strong decrease of intensity for the spectra at intermediate photon energy detunings appear in a range where the interference between the direct and resonant channel is strongly destructive. For larger photon energy detunings (>-1.0 eV) the agreement between numerical and experimental results is better again and the restoring of the vibrational spectrum is well reproduced. This can be rationalized by the fact that in a typical Fano profile there is a minimum in the photoionization cross section on the side of the resonance where destructive interference occurs.

Strictly, a Fano profile is expected in the case of a single resonance, while in the present case, in order to get converged results, the sum in Eq. (2) must include, at least, the lowest ten vibrational levels of the core-excited state. For a given final state, the Fano profile for each one of the ten resonances, considered as isolated, may have destructive interference between direct and resonant process either on the low energy or on the high energy side of the resonance, depending on the relative sign of the direct and resonant amplitude in Eq. (2). This sign, on the other hand, depends also on the several Franck-Condon (FC) amplitudes appearing in Eq. (2). A close scrutiny of such FC amplitudes, in the present case, shows that the characteristic of the several Fano profiles (single resonances) is almost invariably that of having destructive interference on the low energy side of the resonance, corresponding to negative detuning. Due to this peculiarity of the FC amplitudes relevant in the participator
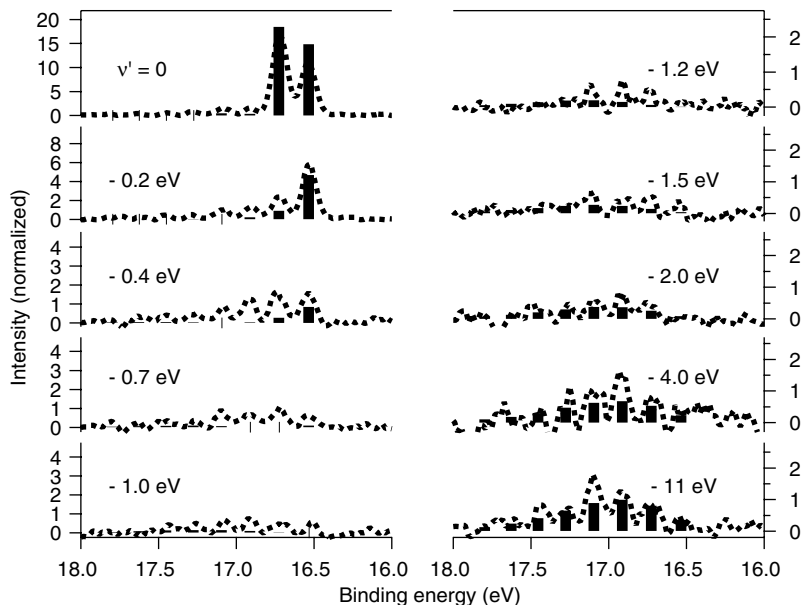

FIG. 3. Comparison of the experimental resonant Auger electron spectra of the $A\,^2\Pi$ state (dotted lines) and results of the numerical simulations adopting a ratio $D/M=0.84$ (bar diagrams).

Auger decay of the O $1s \rightarrow 2\pi$ core-excited state of CO to the A $^2\Pi$ state, the sum over n in Eq. (2) does not average out the asymmetry of the complex, multiresonance, Fano profile and a minimum of the photoionization cross section for negative detuning remains measurable despite the strong lifetime vibrational interference.

IV. SUMMARY

We have measured the evolution of the vibrational intensity distribution of the singly ionized A $^2\Pi$ state when the photon energy is tuned below the adiabatic 0-0 transition of the O $1s \rightarrow 2\pi$ resonance. A strong suppression of the entire vibrational fine structure of this state has been found, leading to its almost complete quenching for certain excitation energies, followed by a partial restoring for larger values of negative photon energy detuning. This behavior could not be explained by the collapse model, which completely neglects the contribution (and interference) of the direct photoionization path to the resonant photoemission process. By numerical simulations of the photoionization cross section considering both the direct and resonant channels, we could show that quenching and restoring of the A $^2\Pi$ vibrational spectra can be understood as a Fano interference betweeen the direct and resonant photoionization channels in the presence of strong lifetime vibrational interference. This finding fits well with our previous study [30] of the Auger resonant Raman spectra of CO, and shows that the photoionization process is more complex for negative photon energy detuning of the radiation than for positive detuning.

[1] T. Åberg and B. Crasemann, in *Resonant Anomalous X-Ray Scattering*, edited by G. Materlik, C. J. Sparks, and K. Fisher (North-Holland, New York, 2004).

[2] A. Kivimäki, A. Naves de Brito, S. Aksela, H. Aksela, O.-P. Sairanen, A. Ausmees, S. J. Osborne, L. B. Dantas, and S. Svensson, Phys. Rev. Lett. **71**, 4307 (1993).

[3] M. N. Piancastelli, J. Electron Spectrosc. Relat. Phenom. **107**, 1 (2000).

[4] S. L. Sorensen and S. Svensson, J. Electron Spectrosc. Relat. Phenom. **114–116**, 1 (2001).

[5] K. Ueda, J. Phys. B **36**, R1 (2003).

[6] J. D. Bozek, S. E. Canton, E. Kukk, and N. Berrah, Chem. Phys. **289**, 149 (2003).

[7] P. Morin and I. Nenner, Phys. Rev. Lett. **56**, 1913 (1986).

[8] O. Björneholm, M. Bässler, A. Ausmees, I. Hjelte, R. Feifel, H. Wang, C. Miron, M. N. Piancastelli, S. Svensson, S. L. Sorensen, F. Gel'mukhanov, and H. Ågren, Phys. Rev. Lett. **84**, 2826 (2000).

[9] K. Ueda, M. Kitajima, A. De Fanis, T. Furuta, H. Shindo, H. Tanaka, K. Okada, R. Feifel, S. L. Sorensen, H. Yoshida, and Y. Senba, Phys. Rev. Lett. **90**, 233006 (2003).

[10] M. Kitajima, K. Ueda, A. De Fanis, T. Furuta, H. Shindo, H. Tanaka, K. Okada, R. Feifel, S. L. Sorensen, F. Gelmukhanov, A. Baev, and H. Ågren, Phys. Rev. Lett. **91**, 213003 (2003).

[11] R. Feifel, F. Burmeister, P. Salek, M. N. Piancastelli, M. Bässler, S. L. Sorensen, C. Miron, H. Wang, I. Hjelte, O. Björneholm, A. Naves de Brito, F. Kh. Gelmukhanov, H. Ågren, and S. Svensson, Phys. Rev. Lett. **85**, 3133 (2000).

[12] F. Gel'mukhanov, L. N. Mazalov, and A. V. Kondratenko, Chem. Phys. Lett. **46**, 133 (1977).

[13] F. Kaspar, W. Domcke, and L. S. Cederbaum, Chem. Phys. **44**, 33 (1979).

[14] J.-E. Rubensson, M. Neeb, M. Biermann, and W. Eberhardt, J. Chem. Phys. **99**, 1633 (1993).

[15] M. Neeb, J.-E. Rubensson, M. Biermann, and W. Eberhardt, J. Electron Spectrosc. Relat. Phenom. **67**, 261 (1994).

[16] S. J. Osborne, A. Ausmess, S. Svensson, A. Kivimäki, O.-P. Sairanen, A. Naves de Brito, H. Aksela, and S. Akesla, J. Chem. Phys. **102**, 7317 (1995).

[17] E. Kukk, J. D. Bozek, W.-T. Cheng, R. F. Fink, A. A. Wills, and N. Berrah, J. Chem. Phys. **111**, 9642 (1999).

[18] S. Sundin, F. K. Gel'mukhanov, H. Ågren, S. J. Osborne, A. Kikas, O. Björneholm, A. Ausmees, and S. Svensson, Phys. Rev. Lett. **79**, 1451 (1997).

[19] F. Gel'mukhanov, T. Privalov, and H. Ågren, Phys. Rev. A **56**, 256 (1997)

[20] R. Feifel, F. Gel'mukhanov, A. Baev, H. Ågren, M.-N. Piancastelli, M. Bässler, C. Miron, S. L. Sorensen, A. Naves de Brito, O. Björneholm, L. Karlsson, and S. Svensson, Phys. Rev. Lett. **89**, 103002 (2002).

[21] A. Baev, R. Feifel, F. Gel'mukhanov, H. Ågren, M.-N. Piancastelli, M. Bässler, C. Miron, S. L. Sorensen, A. Naves de Brito, O. Björneholm, L. Karlsson, and S. Svensson, Phys. Rev. A **67**, 022713 (2003).

[22] F. Gel'mukhanov and H. Ågren, Phys. Rep. **312**, 87 (1999).

[23] U. Fano, Phys. Rev. **124**, 1866 (1961).

[24] R. Camilloni, M. Zitnik, C. Comicioli, K. C. Prince, M. Zacchigna, C. Crotti, C. Ottaviani, C. Quaresima, P. Perfetti, and G. Stefani, Phys. Rev. Lett. **77**, 2646 (1996).

[25] A. De Fanis, N. Saito, H. Yoshida, Y. Senba, Y. Tamenori, H. Ohashi, H. Tanaka, and K. Ueda, Phys. Rev. Lett. **89**, 243001 (2002).

[26] M. N. Piancastelli, M. Neeb, A. Kivimäki, B. Kempgens, H. M. Köppe, K. Maier, and A. M. Bradshaw, Phys. Rev. Lett. **77**, 4302 (1996).

[27] V. Carravetta, F. Kh. Gel'mukhanov, H. Ågren, S. Sundin, S. J.

Osborne, A. Navas de Brito, O. Björneholm, A. Ausmees, and S. Svensson, Phys. Rev. A **56**, 4665 (1997).

[28] V. Carravetta, H. Ågren, O. Vahtras, and H. J. Aa. Jensen, J. Chem. Phys. **113**, 7790 (2000).

[29] M. N. Piancastelli, R. F. Fink, R. Feifel, M. Bässler, S. L. Sorensen, C. Miron, H. Wang, I. Hjelte, Björneholm, P. Salek, F. Kh. Gel'mukhanov, and H. Ågren, J. Phys. B **33**, 1819 (2000).

[30] T. Tanaka, H. Shindo, C. Makochekanwa, M. Kitajima, H. Tanaka, A. De Fanis, Y. Tamenori, K. Okada, R. Feifel, S. Sorensen, E. Kukk, and K. Ueda, Phys. Rev. A **72**, 022507 (2005).

[31] H. Ohashi, E. Ishiguro, Y. Tamenori, H. Kishimoto, M. Tanaka, M. Irie, T. Tanaka, and T. Ishikawa, Nucl. Instrum. Methods Phys. Res. A **467-468**, 529 (2001).

[32] H. Ohashi, E. Ishiguro, Y. Tamenori, H. Okumura, A. Hiraya, H. Yoshida, Y. Senba, K. Okada, N. Saito, I. H. Suzuki, K. Ueda, T. Ibuki, S. Nagaoka, I. Koyano, and T. Ishikawa, Nucl. Instrum. Methods Phys. Res. A **467-468**, 533 (2001).

[33] T. Tanaka and H. Kitamura, Nucl. Instrum. Methods Phys. Res. A **364**, 368 (1995).

[34] T. Tanaka and H. Kitamura, J. Synchrotron Radiat. **3**, 47 (1996).

[35] Y. Shimizu, H. Ohashi, Y. Tamenori, Y. Muramatsu, H. Yoshida, K. Okada, N. Saito, H. Tanaka, I. Koyano, S. Shin, and K. Ueda, J. Electron Spectrosc. Relat. Phenom. **114-116**, 63 (2001).

[36] H. Yoshida, Y. Senba, M. Morita, T. Goya, A. De Fanis, N. Saito, K. Ueda, Y. Tamenori, and H. Ohashi, in *Synchrotron Radiation Instrumentation*, 8th International Conference on Synchrotron Radiation Instrumentation, edited by T. Warwick, J. Arthur, H. A. Padmore, and J. Stöhr, AIP Conf. Proc. No. 705 (AIP, Melville, NY, 2004), p. 267.

[37] R. Püttner, I. Dominguez, T. J. Morgan, C. Cisneros, R. F. Fink, E. Rotenberg, T. Warwick, M. Domke, G. Kaindl, and A. S. Schlachter, Phys. Rev. A **59**, 3415 (1999).

[38] M. Coreno, M. de Simone, K. C. Prince, R. Richter, M. Vondraček, L. Avaldi, and R. Camilloni, Chem. Phys. Lett. **306**, 269 (1999).

[39] B. Wannberg, D. Nordfors, T. K. Tan, L. Karlsson, and L. Mattsson, J. Electron Spectrosc. Relat. Phenom. **47**, 147 (1988).

[40] R. Feifel *et al.* (unpublished).

[41] K. P. Huber and G. Herzberg, *Molecular Spectra and Molecular Structure IV* (Van Nostrand Reinhold, New York, 1979).